

Effects of frequency on electrical fatigue behavior of ZnO-modified

$\text{Pb}(\text{Mg}_{1/3}\text{Nb}_{2/3})_{0.65}\text{Ti}_{0.35}\text{O}_3$ ceramics

Methee Promsawat^{a,*}, Napatporn Promsawat^b, Jenny W. Wong^c, Zhenhua Luo^d,

Soodkhet Pojprapai^e and Sukanda Jiansirisomboon^e

^a*Department of Materials Science and Technology, Faculty of Science, Prince of Songkla University, Hat Yai, Songkhla 90112, Thailand*

^b*Synchrotron Light Research Institute, Muang, Nakhon Ratchasima 30000, Thailand*

^c*Department of Chemistry and 4D LABS, Simon Fraser University, Burnaby, British Columbia V5A 1S6, Canada*

^d*School of Water, Energy and Environment, Cranfield University, Cranfield MK43 0AL, UK*

^e*School of Ceramic Engineering, Suranaree University of Technology, Muang, Nakhon Ratchasima 30000, Thailand*

*Corresponding author. Tel.: +66 74 288365; fax: +66 74 446925.

E-mail address: methee.p@psu.ac.th (M. Promsawat)

Abstract

This work aims to study the effects of frequency on the electrical fatigue behavior of ZnO-modified $\text{Pb}(\text{Mg}_{1/3}\text{Nb}_{2/3})_{0.65}\text{Ti}_{0.35}\text{O}_3$ (PMNT) ceramics. Changes of microstructures, ferroelectric and piezoelectric properties in the ceramics at bipolar electrical fatigue frequencies of 5, 10, 50 and 100 Hz were observed. The thickness of damaged surface in the ceramics decreased with increasing frequency. The degradation of properties in the ceramics fatigued at low frequency was greater than that fatigued at high frequency. The degradation by electrical fatigue at 5 and 10 Hz could be caused by the effects of both field screening and domain pinning, while at higher frequencies the fatigue was mainly a result of the field screening effect. The

fatigue properties of ZnO-modified PMNT ceramics was compared to Pb-based and Pb-free ferroelectric ceramics. It was found that the fatigue endurance of ZnO-modified PMNT ceramic was greater than that of hard PZT ceramic but less than that of Pb-free ferroelectric ceramic.

Keywords: fatigue; ferroelectricity; microstructure; piezoelectricity

1. Introduction

Complex perovskite solid solution $\text{Pb}(\text{Mg}_{1/3}\text{Nb}_{2/3})_{0.65}\text{Ti}_{0.35}\text{O}_3$ (PMNT) is a well-known relaxor-based ferroelectric material that shows excellent electromechanical properties [1,2]. PMNT's extremely high piezoelectric constant and remnant polarization make it a promising material for applications such as piezoelectric actuators, piezoelectric energy harvesters and ferroelectric-based random access memories (Fe-RAMs) [3,4]. In actual applications, these devices will be under repeating electrical loading cycles, which may cause degradation of properties called electrical fatigue.

A decade ago, a large number of researches investigated the electrical fatigue behavior of the well-known lead-based piezoelectric material, $\text{Pb}(\text{Zr,Ti})\text{O}_3$ (PZT), as well as its damage mechanisms due to electrical fatigue [5–8]. It was believed that the electrical fatigue of piezoelectric ceramics was attributed to domain pinning effect, and microcracks arising from large incompatible stress between grains and resultant damages [9,10]. Many publications have reported observation of microcracks in fatigued bulk ferroelectrics [11,12], however, it was unclear whether these microcracks were a consequence of fatigue or a main cause of fatigue. A comprehensive review article on the fatigue of ferroelectric materials was written by Julia Glaum and Mark Hoffman [13]. Recently, there were reports on electrical fatigue behaviors in terms of ferroelectric properties in PMNT and its related materials under a bipolar electric field, in particular in $(1-x)\text{Pb}(\text{Mg}_{1/3}\text{Nb}_{2/3})\text{O}_3-x\text{PbTiO}_3$ [(1-x)PMN-xPT] materials with compositions lying

in the morphotropic phase boundary ($x = 0.30-0.35$) [14,15]. Although there were studies on the effects of experimental parameters such as fatigue loading amplitude on fatigue behaviors of PMN-PT materials [14,16], the frequency effect, which is a significant factor contributing to electrical fatigue degradation, has not yet been well understood. It was reported that fatigue degradation rate increased at lowering fatigue frequency [17]. Majumder *et al.* found that polarization fatigue degradation was proportional to N/f^2 , when N and f represented cycle number and fatigue frequency, respectively [18]. Moreover, Grossmann *et al.* proposed that frequency had an effect on fatigue loss only in the case of incomplete domain switching [19]. It was found in our previous work that 0.4mol%ZnO-modified PMNT ceramics with density of 7.7 g/cm³ (a relative density of 96%) and grain size of 3 μm showed improved ferroelectric and piezoelectric properties [20]. Therefore, 0.4mol%ZnO-modified PMNT ceramic was studied in this work.

In the present work, the effects of electrical frequency on the fatigue behavior of ZnO-modified PMNT ceramics were investigated. In particular, PMNT ceramics modified with 0.4 mol% ZnO were studied. Moreover, fatigue behavior of this ceramic system was compared to Pb-based and Pb-free ferroelectric ceramics [21–24].

2. Experimental procedure

$\text{Pb}(\text{Mg}_{1/3}\text{Nb}_{2/3})_{0.65}\text{Ti}_{0.35}\text{O}_3$ (PMNT) powders were prepared by using PbO, MgO, Nb₂O₅ and TiO₂ powders as precursors. MgNb₂O₆ powders were firstly synthesized and then mixed with predetermined amounts of PbO and TiO₂ powders. The mixed powders were calcined at 850°C for 2 hrs. PMNT powders were mixed with 0.4 mol% ZnO powders and then uniaxially pressed into pellets under ~5.5 MPa pressure. Green bodies were sintered at 1240°C for 2 hrs. The ZnO-modified PMNT ceramics with an average relative density of 96 % were then obtained.

All ceramic samples were cut and polished using 1200 grit SiC paper to a sample dimension of $1.5 \times 3.5 \times 3.0 \text{ mm}^3$. The $3.5 \times 3.0 \text{ mm}^2$ surface of each sample was polished using 5.0, 1.0 and $0.05 \text{ }\mu\text{m}$ alumina powders, sequentially, for a mirror-like surface. All the polished samples were annealed at 500°C for 5 hrs to remove any residual stress due to the polishing process. Electrode was painted on the $3.5 \times 1.5 \text{ mm}^2$ surfaces using a colloidal silver paste (DT1402, Heraeus, USA). The silver-painted samples were cured at 650°C for 15 mins to decompose the organic solvent and increase the bonding strength between the electrode and the sample surfaces. Electrical fatigue tests were performed at frequencies of 5, 10, 50 and 100 Hz. For each fatigue test, a sample was submerged in silicon oil and mounted into a fixture connected to a high voltage supplier (20/20C, Trek, USA). A bipolar sinusoidal electric field with amplitude ± 2 times of the coercive field (equivalent to $\pm 14 \text{ kV/cm}$) was applied across the electroded surfaces of the sample for up to 10^6 cycles. At each fatigue frequency, polarization-electric field (P - E) curves at different cycle numbers (N) were recorded at its cycling frequency by a Sawyer-Tower circuit. For each P - E loop, remnant polarization (P_r) and coercive field (E_c) values were extracted. In order to determine the contribution of domain pinning (reversible) and field screening (irreversible) effects on the fatigue behavior of each frequency ceramic, P - E loops at different states; (I) before fatigue test, (II) at 10^6 cycles fatigue test, (III) after removing damaged surfaces and (IV) after annealing at 500°C for 2 hrs, were recorded. In order to determine the fatigue degradation of piezoelectric properties, percent strain-electric field ($\%Strain$ - E) curves at different N up to 10^5 cycles were recorded by a strain sensor (ZX-TDS01T, OMRON, Japan) in conjunction with the high voltage supplier. For all the fatigue tests, the $\%Strain$ - E curves were measured at a frequency of 50 mHz due to the limitation of the sensor. The $\%S_{\text{total}}$, which was the difference between the maximum and the minimum $\%Strain$, of each $\%Strain$ - E curve was

determined. The piezoelectric constant (d_{33}^*) was determined by the slope of a displacement-voltage curve at zero field (the result was not shown here). In the case of an asymmetric loop, d_{33}^* was averaged from both the positive and negative slopes at zero field. Microstructures of the mirror-like surface for the sample at each frequency were observed via a scanning electron microscope (SEM, JSM-6335F, JEOL, Japan). Moreover, the surface damage in a sample fatigued at 50 Hz, i.e. change of thickness in the damaged layer, was also investigated.

3. Results and discussion

3.1 Microstructures of electrically fatigued ZnO-modified PMNT ceramics

SEM images on the microstructures of the mirror-like surfaces of the samples electrically fatigued at different frequencies for 10^6 cycles were shown in Fig. 1. Microstructural damages on the surfaces by electrical fatigue were observed in all the samples. The observed surface damages are consistent with the results in the previous study [5]. It was also found that electrical fatigue had more pronounced effect on the damage of the surfaces perpendicular to the direction of an applied electric field. This is consistent with a previous observed result in Ref [25]. Besides the damage of the surface underneath the electrode, fatigue induced cracks in the bulk region of the mirror-like surface were observed in the samples fatigued at 5 and 10 Hz, as shown in Fig. 2. The enlarged views of cracks in both of the samples (5 and 10 Hz), as shown in Fig. 2(a) and (b), indicated an intergranular fracture mode. It was also observed that the number and size of the cracks in sample fatigued at the lower frequency sample were greater than those at the higher frequency. Thickness of the damaged layer and size of the cracks, represented by L_D and L_C , respectively, of the ceramics were found to be decreasing with increasing frequency. The L_D values of the samples fatigued at 5, 10, 50 and 100 Hz were equal to 165 ± 7 , 121 ± 5 , 98 ± 4 and 66 ± 4 μm , respectively. The L_C values of the samples fatigued at 5 and 10 Hz were about 45 ± 2

and $19 \pm 1 \text{ } \mu\text{m}$, respectively. We believe the initiation and propagation of cracks are the cause of fatigue degradation in the ferroelectric and piezoelectric properties of the ZnO-modified PMNT ceramics. This will be discussed in the next sections.

3.2 Ferroelectric/piezoelectric properties of electrically fatigued ZnO-modified PMNT ceramics

Polarization-electric field (P - E) curves at different N at the frequencies of 5, 10, 50 and 100 Hz were measured. To obtain the same ferroelectric response as fatigue test, the frequency of the P - E loop measurement was the same as the fatigue frequency. Ferroelectric property parameters, i.e. remnant polarization (P_r) and coercive field (E_c), measured at different N were normalized to those measured before fatigue test. Plots of normalized P_r and normalized E_c as a function of N were shown in Fig. 3(a) and (b), respectively. At $N \leq 10^3$ cycles, the normalized P_r and E_c of all samples did not change with the cycle number. However, the normalized P_r tended to decrease with further increase of N up to 10^6 cycles. The normalized E_c increased with increasing N up to 10^5 cycles and then decreased with further increasing of N up to 10^6 cycles. However, for the samples fatigued at 5 and 10 Hz, the normalized E_c did not decrease further when $N \geq 4 \times 10^5$ cycles. As observed in previous works, the electrical fatigue degradation was attributed by field screening caused by surface damages and domain pinning effects [9, 26, 27], which will be described in the next parts.

In order to determine the causes of the fatigue degradations of the ceramics, P - E loops at different states; (I) at the beginning of fatigue test, (II) after fatigue testing for 10^6 cycles, (III) after removing the damaged layers and (IV) after annealing at $500 \text{ } ^\circ\text{C}$ for 2 hrs, were shown in Fig. 4. The P - E loops of the samples fatigued at all frequencies at state II were more restricted, at which P_r values were much lower than those measured at state I. At State III, the P - E loops of the samples fatigued at 50 and 100 Hz were completely recovered after removing the damaged

layers. However, P - E loops of the samples fatigued at 5 and 10 Hz did not recover completely using the same technique. At State IV after the thermal annealing, the P - E loop of the sample fatigued at 10 Hz was completely recovered while that of the sample fatigued at 5 Hz was only partly recovered. Incomplete recovering of the P - E loop of the sample fatigued at 5 Hz was due to the fatigue induced cracks, which were more and larger compared to others. Nevertheless, the cracks in the sample fatigued at 10 Hz were less and smaller. Hence, the P - E loops of the sample were less difficult to be recovered by layer removal and thermal annealing.

Moreover, in order to determine the relationship between the damaged layers and the change of ferroelectric properties, cycle number dependences of the damaged layers' thickness, P_r and E_c of the sample fatigued at 50 Hz were observed, as shown in Fig. 5. At $N \leq 10^5$ cycles, the increased thickness of damaged layer resulted in a decrease in P_r and an increase in E_c . At $N > 10^5$ cycles, the thickness of damaged layer only increased very slightly. At this cycle number range, P_r continued to decrease while E_c started decreasing with increasing N to 10^6 cycles.

Fatigue induced degradation cycle number of ferroelectric properties, i.e. the cycle number at which the degradation rate of normalized P_r is maximum, was determined from the experiments and given in Table 1. Degradation cycle number increased with increasing frequency. This implied faster initiations of fatigue degradations in samples fatigued at lower frequency. The % changes of the properties after 10^5 cycles of fatigue tests compared to those at the beginning of the tests were determined and given in Table 1. The magnitude of the degradation of ferroelectric properties tended to decrease with increasing frequency. It indicated that the severity of fatigue degradation of ferroelectric properties in the ceramics decreased with increasing fatigue frequency.

3.3 Electric field-induced strain of electrically fatigued ZnO-modified PMNT bulk samples

Strain versus electric field (S - E) butterfly-loops of the samples fatigued at 5, 10, 50 and 100 Hz, were measured at different N cycles up to 10^5 cycles, as shown in Fig. 6. For all the samples, their S - E loops fatigued for 10^5 cycles were asymmetric, illustrating incomplete domain switching. For each sample, a total strain ($\%S_{\text{total}}$) was determined by the difference between the maximum ($\%S_{\text{max}}$) and the minimum ($\%S_{\text{min}}$) strains. Moreover, d_{33}^* value was determined by the slope at zero voltage in the displacement versus voltage curve (the result is not shown here). The d_{33}^* value measured before fatigue was equal to 1700 pm/V. $\%S_{\text{total}}$ and d_{33}^* values of the samples fatigued after 10^5 cycles were compared to those measured at the beginning of fatigue test. Plots of changes in $\%S_{\text{total}}$ and d_{33}^* as a function of frequency were shown in Fig. 7(a). As frequency increased, the changes in $\%S_{\text{total}}$ and d_{33}^* decreased.

The $\%$ changes in P_r and E_c after fatigue for 10^6 cycles in the sample fatigued at 10 Hz were compared to lead-based and lead-free ferroelectrics as shown in Table 3. The changes in ferroelectric properties of ZnO-modified PMNT ceramics were greater than those of La-doped $\text{Pb}(\text{Mg}_{1/3}\text{Nb}_{2/3})\text{O}_3$ (PMN) ceramics [9]. The change in P_r was not significantly different from that of $0.675\text{Pb}(\text{Mg}_{1/3}\text{Nb}_{2/3})\text{O}_3$ - 0.325PbTiO_3 (0.675PMN-0.325PT) ceramic [15], but the change in E_c was much lower. Moreover, the fatigue endurance of the ceramics in our work were greater than that of a commercial PZT ceramic [28]. On the other hand, comparing to lead-free materials, i.e. $0.025\text{Bi}(\text{Mg}_{1/2}\text{Ti}_{1/2})\text{O}_3$ - $0.40(\text{Bi}_{1/2}\text{K}_{1/2})\text{TiO}_3$ - $0.575(\text{Bi}_{1/2}\text{Na}_{1/2})\text{TiO}_3$ (2.5BMT-40BKT-57.5BNT) [24], SrTiO_3 -modified $\text{Bi}_{0.5}\text{Na}_{0.5}\text{TiO}_3$ - BaTiO_3 (ST-modified BNT-BT) [29] and CaZrO_3 -modified $(\text{K}_{0.49}\text{Na}_{0.49}\text{Li}_{0.02})(\text{Ta}_{0.2}\text{Nb}_{0.8})\text{O}_3$ (CZr-modified KNN) [30], ZnO-modified PMNT ceramics showed greater change in ferroelectric properties. This indicated that the fatigue endurance of ZnO-modified PMNT ceramic was lower than that of lead-free materials.

3.3 Discussion

During an application of a cycling electric field, some domain walls did not move following the change of the field's direction. This might be attributed to microscopic defects within grains which reduce the mobility of domain walls [31], causing the formation of internal stresses. Surface damage can be originated at these points when stress intensity reached the mechanical fracture toughness (K_{IC}) of the materials [32,33]. In the case of lowcycling frequencies, domains experienced a longer time under local electric field in a single cycle, which promoted domain wall movements. As a result, greater stress intensities were produced, enhancing degree of surface damages. It was confirmed by the higher value of P_r of the P - E loops measured at lower frequencies, which was an indication of greater domain wall movements, as shown in Fig. 7(b). For samples fatigued at 5 and 10 Hz, due to the large local stresses with high intensities were produced, fatigue induced cracks were produced as a result.

From Fig. 4, the fatigue observed in samples fatigued at 50 and 100 Hz was mainly attributed to the surface damages (the irreversible process), since their P - E loops were able to recover after removing damaged layers. The recovery of P - E loops by the removal of damaged layers was incomplete in the samples fatigued at 5 and 10 Hz. This indicated that the degradation of ferroelectric properties due to the fatigue at 5 and 10 Hz was also attributed by the domain pinning effect (the reversible process). Under electric field at low cycling frequency, charged defects such as oxygen vacancies could move to local interfaces, i.e. domain walls, and obstructed domains from switching, resulting in a degradation of ferroelectric properties [34]. When thermally annealed, the P - E loop of the sample fatigued at 10 Hz was completely recovered. However, the P - E loop of the sample fatigued at 5 Hz only improved slightly after the sample was thermally annealed. This could be caused by the presence of the large sized cracks

formed by the fatigue. From above discussion, greater microstructural damages, i.e. the damage of the electroded surfaces and the fatigue induced cracks, were resulted under lower cycling frequency, attributing to the larger degradation of ferroelectric and piezoelectric properties, i.e. a decrease in P_r , $\%S_{\text{total}}$ and d_{33}^* , and an increase in E_c , of the materials.

As shown in Fig. 5, at $N \leq 10^5$ cycles, the drop of P_r with decreasing E_c was attributed to the formation of damaged layers that had low ferroelectricity and dielectric properties, i.e. a low P_r , a high E_c and a low dielectric constant [35]. It should be noted that at this range of cycle number the screened electric field from field screening effect was still higher than the E_c of the material, thus promoting a complete domain switching. At $N > 10^5$ cycles, although the thickness of the damaged layer only increased slightly, it was believed that microcracks could be formed by fatigue at such large cycle numbers. Therefore, at $N > 10^5$ cycles, the applied field was screened by both the damaged layers and the microcracks. This caused the decrease in the amplitude of the field acting on the undamaged layer. The field amplitude could be lower than the E_c of the material. An application of the electric field with such amplitude resulted in incomplete switching of the domains in the undamaged layer, thereby leading to the lowered P_r of the ceramic. Moreover, the incomplete switching of the domains also resulted in the lowered interaction strength between the domains. Subsequently, the material required a lower amplitude of the field used for switching its domains, resulting in the decrease in E_c of the ceramic.

It was proposed by Lou that the factors influenced on the fatigue behaviors of ferroelectric ceramics include: (i) type of electrode material, (ii) quality of material-electrode interface, (iii) crystal structure of material, (iv) crystal microstructure including composition, grain size and porosity, (v) doping with other elements, (vi) processing conditions used in fabrication of material and (vii) direction of property measurement in respect to fatigue cycling

direction [36]. From the comparison in Table 2, different fatigue behaviors of ZnO-modified PMNT ceramics and the PZT ceramic could be caused by their difference in crystal structure. The PZT ceramic has a tetragonal phase (K350, Piezo Technologies, Indianapolis, IN, USA) while the ZnO-modified PMNT ceramic has a combination of monoclinic and tetragonal phases [20]. For PMN-based materials, a greater fatigue degradation could be caused by the higher degree of tetragonality. This was supported by an observed result investigated by Jiang *et al.*, where the fatigue degradations of materials with a rhombohedral symmetry were much lower than those of materials with tetragonal or orthorhombic symmetries [9]. The excellent fatigue endurance of lead-free ceramics could be due to a low concentration of intrinsic defects such as cation and anion vacancies [23], an increase in ergodicity and a lack of induced tetragonality during fatigue cycles [37]. From the comparison, the fatigue resistance of the ZnO-modified PMNT ceramic was slightly greater than that of a soft PZT ceramic, but poorer than that of the lead-free piezoelectric ceramics. Therefore, for the applications such as actuators and FRAMs, the fatigue endurance of ZnO-modified PMNT need to be further improved, which required further investigation. .

4. Conclusions

Electrical fatigue tests on ZnO-modified $\text{Pb}(\text{Mg}_{1/3}\text{Nb}_{2/3})_{0.65}\text{Ti}_{0.35}\text{O}_3$ ceramics at frequencies of 5, 10, 50 and 100 Hz were studied. Surface damages underneath the electrodes were observed in all samples, while electrical fatigue induced cracks in the bulk were only observed in the samples fatigued at 5 and 10 Hz. Thickness of the damaged layers and size of the cracks decreased with increasing frequency. Fatigue degradations in samples at lower frequencies were initiated faster than those at higher frequencies. The changes of P_r , E_c , %Strain and d_{33}^* decreased with increasing frequency. Local fatigue induced strain by the applied electric

fields was reduced with an increase in frequency. This contributed to the lowering degree of fatigue induced surface damages and, consequently, less degradations of properties. Fatigue behaviors of the samples at low frequency could be caused by both reversible (domain pinning effect) and irreversible (surfaces damage) processes. At high frequency, the irreversible process had more pronounced effect on the fatigue behaviors. The fatigue endurance of ZnO-modified PMNT ceramic was slightly greater than that of a PZT ceramic but poorer than that of monolithic PMN and lead-free piezoelectric ceramics. Therefore, further development is needed on the crystal structure and microstructure of ZnO-modified PMNT in order to use it for actuator and FERM applications.

Acknowledgements

This research was supported by Natural Rubber Innovation Research Institute, Prince of Songkla University (Grant No. SCI601093S). SP and SJ would like to thank the Thailand Research Fund (TRF). SP would also like to thank Newton Fund.

References

- [1] M. Alguero, A. Moure, J. Pardo, J. Holc, M. Kosec, Processing by mechano synthesis and properties of piezoelectric $\text{Pb}(\text{Mg}_{1/3}\text{Nb}_{2/3})\text{O}_3\text{-PbTiO}_3$ with different compositions, *Acta Mater.* 54 (2006) 501–511.
- [2] Z.-G. Ye, High-performance piezoelectric single crystals of complex perovskite solid solutions, *Mater. Res. Bull.* 34 (2009) 277–283.
- [3] Y. Chen, K. H. Lam, D. Zhou, W. F. Cheng, J. Y. Dai, H. S. Luo, H. L. W. Chan, High frequency PMN-PT single crystal focusing transducer fabricated by a mechanical dimpling technique, *Ultrasonics* 53 (2013) 345–349.

- [4] G.-T. Hwang, H. Park, J.-H. Lee, S. Oh, K.-I Park, M. Byun, H. Park, G. Ahn, C. K. Jeong, K. No, H.-S. Kwon, S.-G. Lee, B. Joung, K. J. Lee, Self-powered cardiac pacemaker enabled by flexible single crystalline PMN-PT piezoelectric energy harvester, *Adv. Mater.* 26 (2014) 4880–4887.
- [5] N. Balke, H. Kungl, T. Granzow, D. C. Lupascu, M. J. Hoffmann, J. Rödel, Bipolar fatigue caused by field screening in $\text{Pb}(\text{Zr,Ti})\text{O}_3$ ceramics, *J. Am. Ceram. Soc.* 90 (2007) 3869–3874.
- [6] J. Glaum, T. Granzow, J. Rödel, Evaluation of domain wall motion in bipolar fatigued lead-zirconate-titanate: A study on reversible and irreversible contributions, *J. Appl. Phys.* 107 (2010) 104119/1–6.
- [7] F. W. Zeng, H. Wang, H. Lin, Fatigue and failure response of lead zirconate titanate multilayer actuator under unipolar high-field electric cycling fatigue, *J. Appl. Phys.* 114 (2013) 024101/1–9.
- [8] D. A. Hall, T. Mori, T. P. Comyn, E. Ringgaard, J. P. Wright, Residual stress relief due to fatigue in tetragonal lead zirconate titanate ceramics, *J. Appl. Phys.* 114 (2013) 024101/1–9.
- [9] Q. Y. Jiang, E. C. Subbarao, L. E. Cross, Effect of composition and temperature on electric fatigue of La-doped lead zirconate titanate ceramics, *J. Appl. Phys.* 75 (1994) 7433–7443.
- [10] L. Jin, F. Li, S. Zhang, Decoding the fingerprint of ferroelectric loops: comprehension of the material properties and structures, *J. Am. Ceram. Soc.* 97 (2014) 1–27.
- [11] J. Nuffer, D. C. Lupascu, J. Rödel, Microcrack clouds in fatigued electrostrictive 9.5/65/35 PLZT, *J. Eur. Ceram. Soc.* 21 (2001) 1421–1423.

- [12] J. Nuffer, D. C. Lupascu, A. Glazounov, H. J. Kleebe, J. Rödel, Microstructural modifications of ferroelectric lead zirconate titanate ceramics due to bipolar electric fatigue, *J. Eur. Ceram. Soc.* 22 (2002) 2133–2142.
- [13] J. Glaum, M. Hoffman, Electric fatigue of lead-free piezoelectric materials, *J. Am. Ceram. Soc.* 97 (2014) 665–680.
- [14] D. Lin, Z. Li, Z.-Y. Cheng, Z. Xu, X. Yao, Electric-field-induced polarization fatigue of [001]-oriented $\text{Pb}(\text{Mg}_{1/3}\text{Nb}_{2/3})\text{O}_3$ -0.32 PbTiO_3 single crystals, *Solid State Commun.* 151 (2011) 1188–1191.
- [15] Y. Yan, Y. Zhou, S. Gupta, S. Priya, Fatigue mechanism of textured $\text{Pb}(\text{Mg}_{1/3}\text{Nb}_{2/3})\text{O}_3$ - PbTiO_3 ceramics, *Appl. Phys. Lett.* 103 (2013) 082906/1–5.
- [16] E. A. McLaughlin, T. Liu, C. S. Lynch, Relaxor ferroelectric PMN-32%PT crystals under stress and electric field loading: I-32 mode measurements, *Acta Mater.* 52 (2004) 3849–3857.
- [17] K. Lee, B. R. Rhee, C. Lee, Characteristics of ferroelectric $\text{Pb}(\text{Zr,Ti})\text{O}_3$ thin films having Pt/PtO_x electrode barriers, *Appl. Phys. Lett.* 79 (2001) 821–823.
- [18] S. B. Majumder, Y. N. Mohapatra, D. C. Agrawal, Fatigue resistance in lead zirconate titanate thin ferroelectric films: effect of cerium doping and frequency dependence, *Appl. Phys. Lett.* 70 (1997) 138–140.
- [19] M. Grossmann, D. Bolten, O. Lohse, U. Boettger, R. Waser, S. Tiedke, Correlation between switching and fatigue in $\text{PbZr}_{0.3}\text{Ti}_{0.7}\text{O}_3$ thin films, *Appl. Phys. Lett.* 77 (2000) 1894–1896.

- [20] M. Promsawat, A. Watcharapasorn, Z.-G. Ye, S. Jiansirisomboon, Enhanced dielectric and ferroelectric properties of $\text{Pb}(\text{Mg}_{1/3}\text{Nb}_{2/3})_{0.65}\text{Ti}_{0.35}\text{O}_3$ ceramics by ZnO modification, *J. Am. Ceram. Soc.* 98 (2015) 848–854.
- [21] S. Pojprapai, J. Russell, H. Man, J. L. Jones, J. E. Daniels, M. Hoffman, Frequency effects on fatigue crack growth and crack tip domain-switching behavior in a lead zirconate titanate ceramic, *Acta Mater.* 57 (2009) 3932–3940.
- [22] Z. Luo, J. Glaum, T. Granzow, W. Jo, R. Dittmer, M. Hoffman, J. Rödel, Bipolar and unipolar fatigue of ferroelectric BNT-based lead-free piezoceramics, *J. Am. Ceram. Soc.* 94 (2011) 529–535.
- [23] E. A. Patterson, D. P. Cann, Bipolar piezoelectric fatigue of $\text{Bi}(\text{Zn}_{0.5}\text{Ti}_{0.5})\text{O}_3$ - $(\text{Bi}_{0.5}\text{K}_{0.5})\text{TiO}_3$ - $(\text{Bi}_{0.5}\text{Na}_{0.5})\text{TiO}_3$ Pb-free ceramics, *Appl. Phys. Lett.* 101 (2012) 042905/1–6.
- [24] N. Kumar, D. P. Cann, Electromechanical strain and bipolar fatigue in $\text{Bi}(\text{Mg}_{1/2}\text{Ti}_{1/2})\text{O}_3$ - $(\text{Bi}_{1/2}\text{K}_{1/2})\text{TiO}_3$ - $(\text{Bi}_{1/2}\text{Na}_{1/2})\text{TiO}_3$ ceramics, *J. Appl. Phys.* 114 (2013) 054102/1–6.
- [25] D. N. Fang, Y. H. Zhang, G. Z. Mao, Electric-field-induced fatigue crack growth in ferroelectric ceramics, *Theor. Appl. Fract. Mech.* 54 (2010) 98–104.
- [26] C. Brennan, Model of ferroelectric fatigue due to defect/domain interactions, *Ferroelectrics* 150 (1993) 199–208.
- [27] J. Glaum, T. Granzow, L. A. Schmitt, H. J. Kleebe, J. Rödel, Temperature and driving field dependence of fatigue processes in PZT bulk ceramics, *Acta Mater.* 59 (2011) 6083–6092.
- [28] Z. Luo, S. Pojprapai, J. Glaum, M. Hoffman, Electrical fatigue-induced cracking in lead zirconate titanate piezoelectric ceramic and its influence quantitatively analyzed by refatigue method, *J. Am. Ceram. Soc.* 95 (2012) 2593–2600.

- [29] C. Tian, F. Wang, X. Ye, Y. Xie, T. Wang, Y. Tang, D. Sun, W. Shi, Bipolar fatigue-resistant behavior in ternary $\text{Bi}_{0.5}\text{Na}_{0.5}\text{TiO}_3\text{-BaTiO}_3\text{-SrTiO}_3$ solid solutions, *Scr. Mater.* 83 (2014) 25–28.
- [30] F.-Z. Yao, E. A. Patterson, K. Wang, W. Jo, J. Rödel, J.-F. Li, Enhanced bipolar fatigue resistance in CaZrO_3 -modified $(\text{K},\text{Na})\text{NbO}_3$ lead-free piezoceramics, *Appl. Phys. Lett.* 104 (2014) 242912/1–5.
- [31] D. Lupascu, J. Rödel, Fatigue in bulk lead zirconate titanate actuator materials, *Adv. Eng. Mater.* 7 (2005) 882–898.
- [32] Q. Y. Jiang, E. C. Subbarao, L. E. Cross, Grain size dependence of electric fatigue behavior of hot pressed PLZT ferroelectric ceramics, *Acta. Metall. Mater.* 42 (1994) 3687–3694.
- [33] J. Shieh, J. E. Huber, N. A. Fleck, Fatigue crack growth in ferroelectrics under electrical loading, *J. Euro. Ceram. Soc.* 26 (2006) 95–109.
- [34] Y. A. Genenko, J. Glaum, M. J. Hoffmann, K. Albe, Mechanisms of aging and fatigue in ferroelectrics, *Mater. Sci. Eng. B* 192 (2015) 52–82.
- [35] W. Li, R. M. McMeeking, C. M. Landis, On the crack face boundary conditions in electromechanical fracture and an experimental protocol for determining energy release rates, *Eur. J. Mech. A. Solids* 27 (2008) 285–301.
- [36] X. J. Lou, Polarization fatigue in ferroelectric thin films and related materials, *J. Appl. Phys.* 105 (2009) 024101/1–24.
- [37] N. Kumar, T. Y. Ansell, D. P. Cann, Role of point defects in bipolar fatigue behavior of $\text{Bi}(\text{Mg}_{1/2}\text{Ti}_{1/2})\text{O}_3$ modified $(\text{Bi}_{1/2}\text{K}_{1/2})\text{TiO}_3\text{-(Bi}_{1/2}\text{Na}_{1/2})\text{TiO}_3$ relaxor ceramics, *J. Appl. Phys.* 115 (2014) 154104/1–9.

Figure captions

Fig. 1. SEM images of surfaces near an electrode layer of samples fatigued at (a) 5, (b) 10, (c) 50 and (d) 100 Hz for 10^6 cycles. Damaged layer thickness is denoted as L_D .

Fig. 2. SEM images of mirror-like surfaces of samples fatigued for 10^6 cycles at (a) 5 and (b) 10 Hz. Electric field induced-cracks are indicated by the arrows. Enlarged views of a crack observed in samples fatigued at 5 and 10 Hz are shown in (c) and (d), respectively. Crack width is denoted as L_C .

Fig. 3. Plots of (a) normalized remnant polarization and (b) normalized coercive field as a function of cyclic number of the samples under bipolar electric fields with an amplitude of ± 14 kV/cm at frequencies of 5, 10, 50 and 100 Hz.

Fig. 4. P - E loops measured (I) before fatigue test, (II) at 10^6 cycles fatigue test, (III) after removing the damaged layers and (IV) after annealing at 500 °C for 2 hrs of the samples fatigued at (a) 5, (b) 10, (c) 50 and (d) 100 Hz.

Fig. 5. Plots of damaged layer thickness, remnant polarization and coercive field as a function of cycle number of ZnO-modified PMNT ceramic fatigued at 50 Hz.

Fig. 6. %*Strain* versus electric field loops measured at different cycle numbers of the samples fatigued at (a) 5, (b) 10, (c) 50 and (d) 100 Hz.

Fig. 7. (a) Plots of percent decrease in % S_{total} and d_{33}^* as a function of fatigue frequencies and (b) P - E loops measured at frequencies of 5, 10, 50 and 100 Hz of an unfatigued sample.

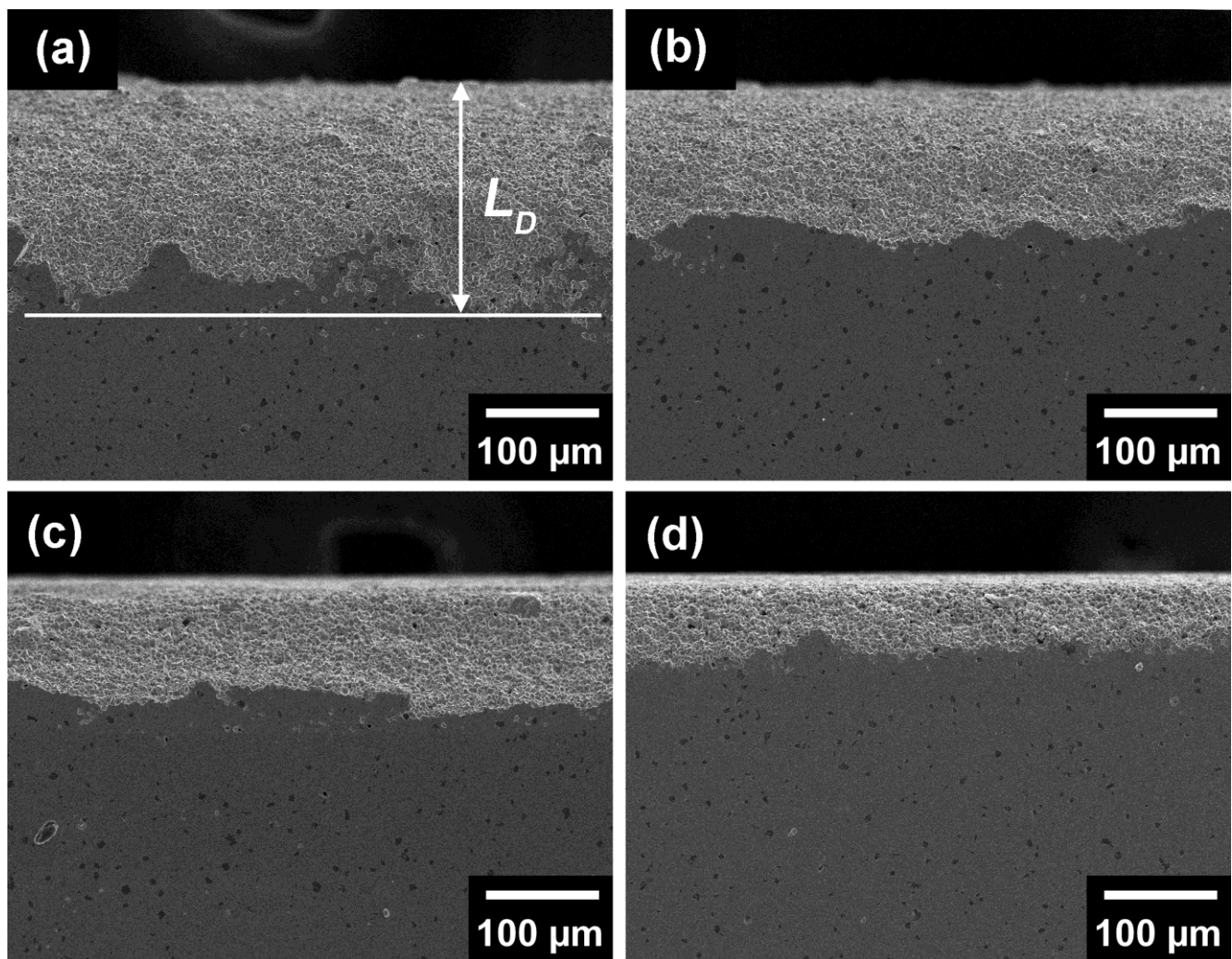


Fig. 1. SEM images of surfaces near an electrode layer of samples fatigued at (a) 5, (b) 10, (c) 50 and (d) 100 Hz for 10^6 cycles. Damaged layer thickness is denoted as L_D .

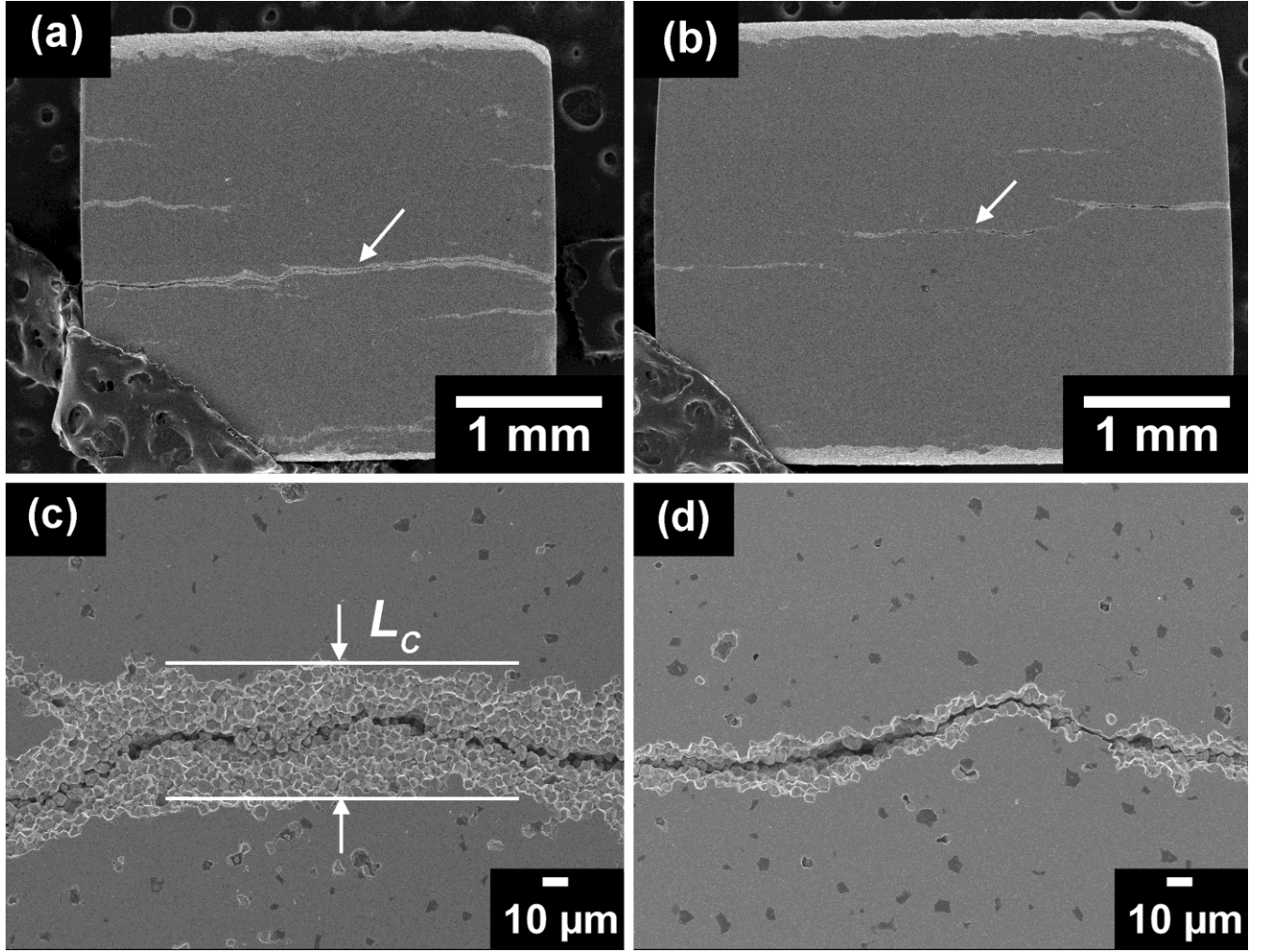


Fig. 2. SEM images of mirror-like surfaces of samples fatigued for 10^6 cycles at (a) 5 and (b) 10 Hz. Electric field induced-cracks are indicated by the arrows. Enlarged views of a crack observed in samples fatigued at 5 and 10 Hz are shown in (c) and (d), respectively. Crack width is denoted as L_C .

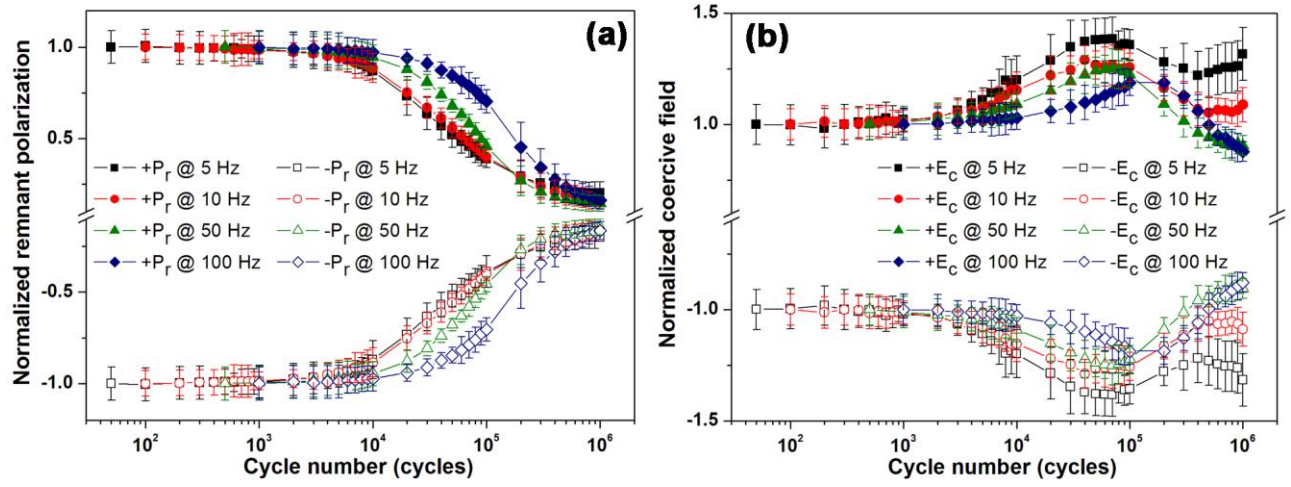


Fig. 3. Plots of (a) normalized remnant polarization and (b) normalized coercive field as a function of cyclic number of the samples under bipolar electric fields with an amplitude of ± 14 kV/cm at frequencies of 5, 10, 50 and 100 Hz.

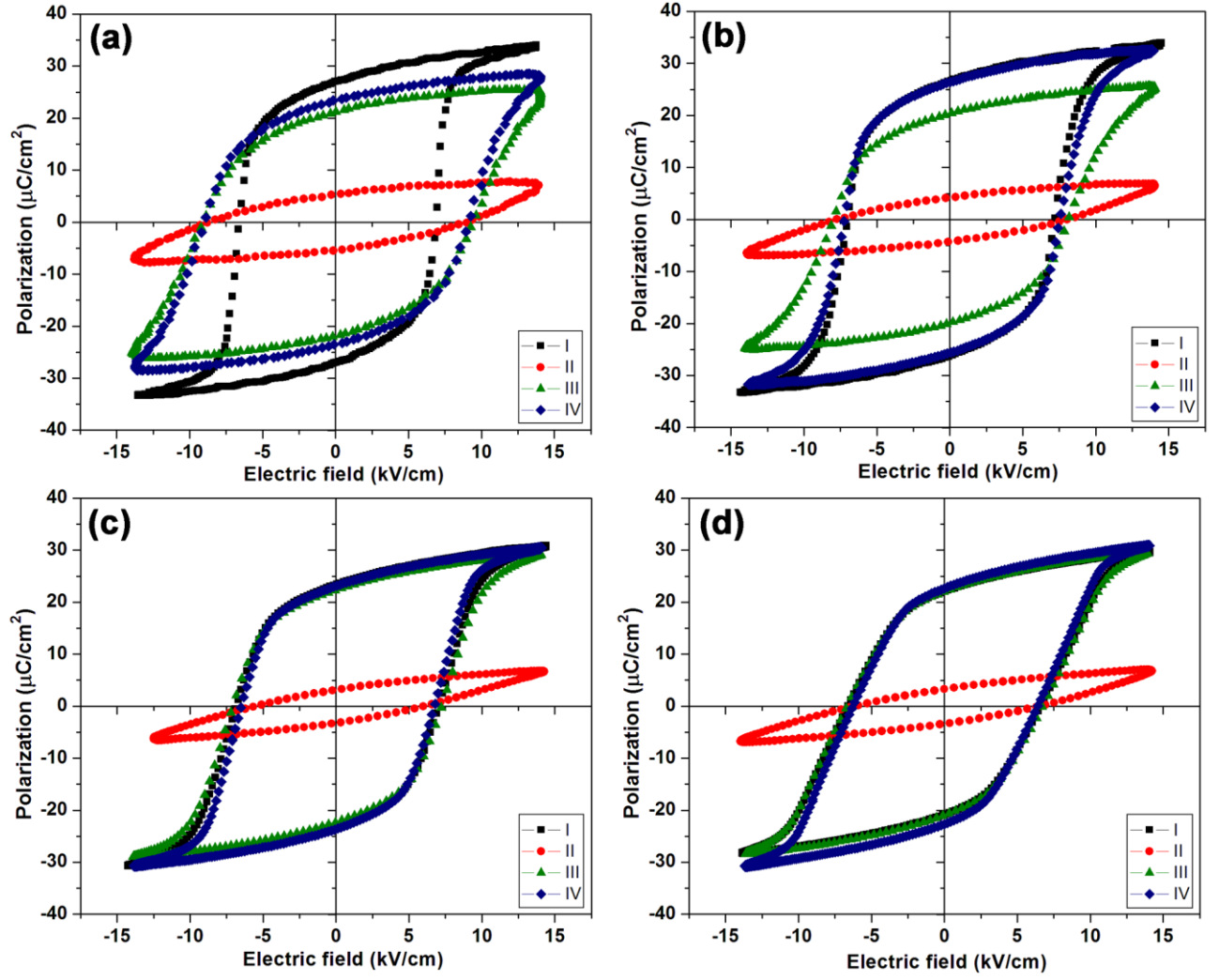


Fig. 4. P - E loops measured (I) before fatigue test, (II) at 10^6 cycles fatigue test, (III) after removing the damaged layers and (IV) after annealing at 500°C for 2 hrs of the samples fatigued at (a) 5, (b) 10, (c) 50 and (d) 100 Hz.

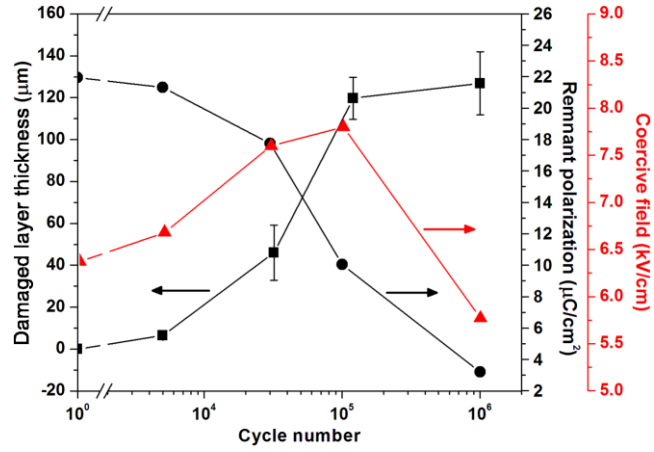


Fig. 5. Plots of damaged layer thickness, remnant polarization and coercive field as a function of cycle number of ZnO-modified PMNT ceramic fatigued at 50 Hz.

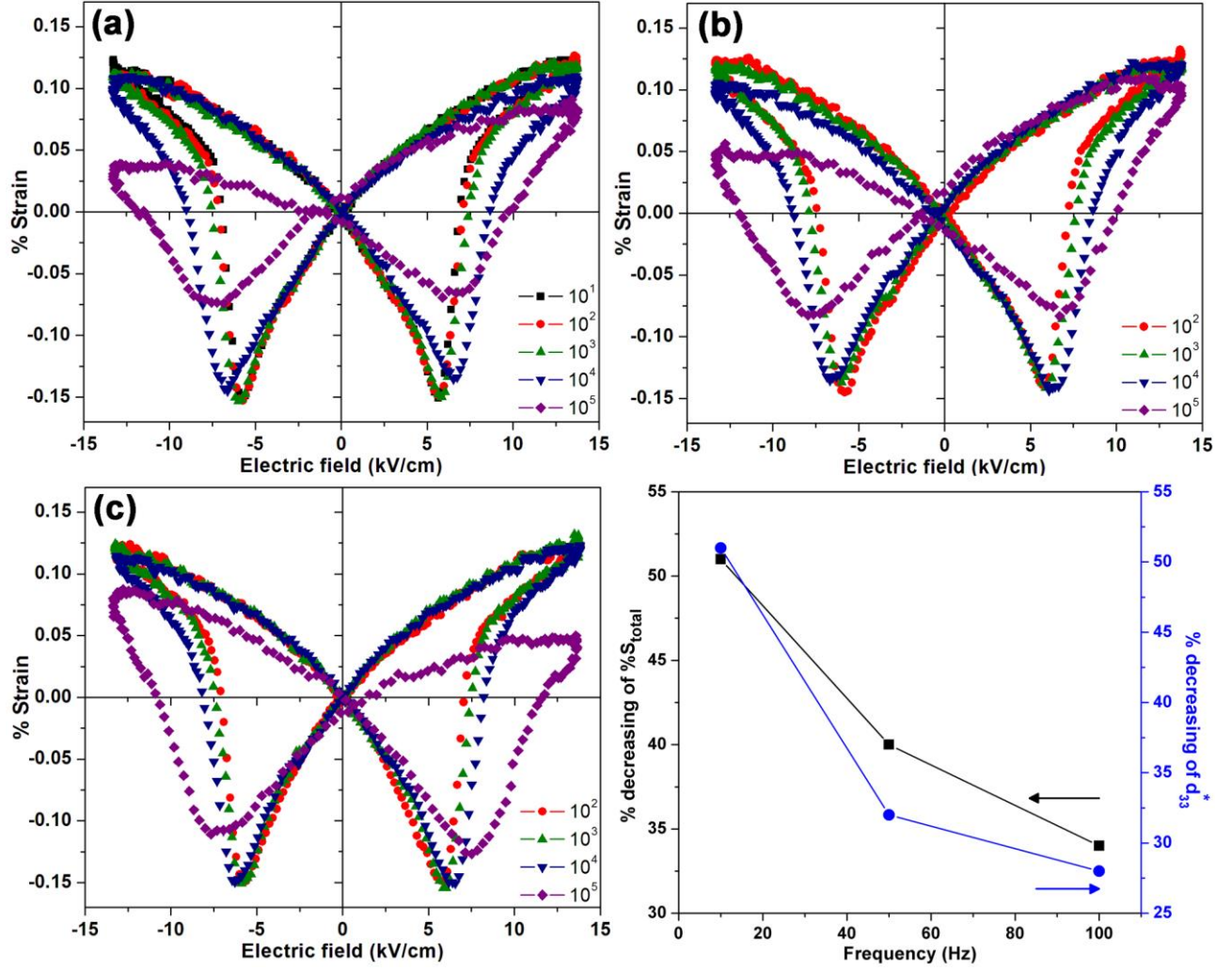


Fig. 6. %Strain versus electric field loops measured at different cycle numbers of the samples fatigued at (a) 10, (b) 50 and (c) 100 Hz. (d) Plots of percent decrease in $\%S_{\text{total}}$ and d_{33}^* as a function of fatigue frequencies of ZnO-modified PMNT ceramics.

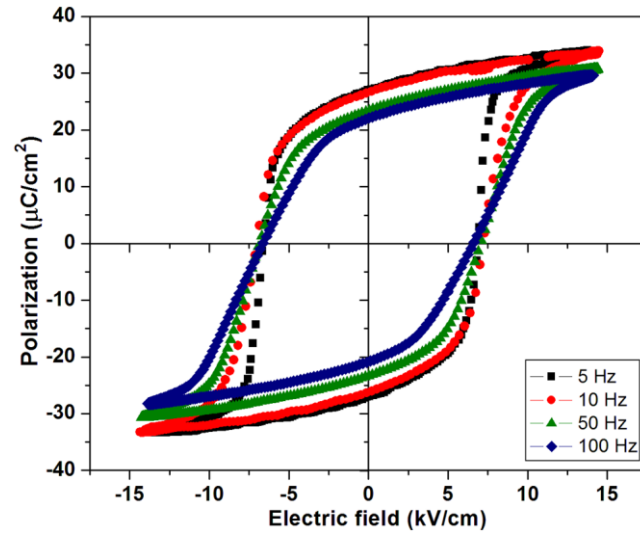


Fig. 7. P - E loops measured at frequencies of 5, 10, 50 and 100 Hz of an unfatigued sample.

Table 1 Electrical fatigue behaviors of ferroelectric properties after fatigue testing for 10^5 cycles at different frequencies of ZnO-modified PMNT ceramics.

Frequency (Hz)	N (cycles)	%change in normalized P_r	%change in normalized E_c
5	30000	-61	+36
10	63000	-60	+26
50	86000	-54	+22
100	140000	-29	+19

Note: N represents the cycle number at which the normalized P_r decreases.

Table 2 Percent changes in remnant polarization and coercive field of ZnO-modified PMNT ceramics compared with those of lead-based and lead-free ferroelectric ceramics available in the literature.

Material	Cycling frequency, field*	Cycle numbers	%change in P_r	%change in E_c	References
ZnO-modified PMNT	10 Hz, $2E_c$	10^6	-83	+9	This work
1%La-doped PMN	-	10^6	-1	0	[9]
0.675PMN-0.325PT	10 Hz, $3E_c$	10^6	-72	+82	[14]
PZT	10 Hz, $2E_c$	5×10^5	-63	+49	[27]
2.5BMT-40BKT-57.5BNT	10 Hz, $3.3E_c$	10^6	-1	-2	[23]
ST-modified BNT-BT	10 Hz, $2E_c$	10^6	-1	-23	[28]
CZr-modified KNN	50 Hz, $2E_c$	10^6	-6	-4	[29]

* The maximum electric field is in multiples of the coercive field.

Effects of frequency on electrical fatigue behavior of ZnO-modified Pb(Mg_{1/3}Nb_{2/3})_{0.65}Ti_{0.35}O₃ ceramics

Promsawat, Methee

2017-07-08

Attribution-NonCommercial-NoDerivatives 4.0 International

Promsawat M, Promsawat N, Wong JW, Luo Z, Pojprapai S, Jiansirisomboon S, Effects of frequency on electrical fatigue behavior of ZnO-modified Pb(Mg_{1/3}Nb_{2/3})_{0.65}Ti_{0.35}O₃ ceramics, *Ceramics International*, Vol. 43, Issue 16, November 2017, pp. 13475-13482

<http://dx.doi.org/10.1016/j.ceramint.2017.07.052>

Downloaded from CERES Research Repository, Cranfield University